

Supersaturated N₂O in a perennially ice-covered Antarctic lake: Molecular and stable isotopic evidence for a biogeochemical relict

*John C. Priscu*¹

Montana State University, Department of Land Resources and Environmental Sciences, Bozeman, Montana 59717

Brent C. Christner

Louisiana State University, Department of Biological Sciences, Baton Rouge, Louisiana 70803

John E. Dore

Montana State University, Department of Land Resources and Environmental Sciences, Bozeman, Montana 59717
University of Hawaii, Department of Oceanography, School of Ocean and Earth Science and Technology, Honolulu, Hawaii 96822

Marian B. Westley

University of Hawaii, Department of Oceanography, School of Ocean and Earth Science and Technology, Honolulu, Hawaii 96822

Brian N. Popp

University of Hawaii, Department of Geology and Geophysics, School of Ocean and Earth Science and Technology, Honolulu, Hawaii 96822

Karen L. Casciotti

Woods Hole Oceanographic Institution, Department of Marine Chemistry and Geochemistry, Woods Hole, Massachusetts 02543

W. Berry Lyons

Byrd Polar Research Center and School of Earth Sciences, Ohio State University, Columbus, Ohio 43210

Abstract

The east lobe of Lake Bonney, a permanently ice-covered lake in the McMurdo Dry Valleys, Antarctica, has a mid-depth maximum N₂O concentration of 43.3 μmol N L⁻¹ (>700,000% saturation with respect to air), representing one of the highest concentrations reported for a natural aquatic system. δ¹⁵N and δ¹⁸O measurements indicate that this is the most isotopically depleted N₂O yet observed in a natural environment (minimum δ¹⁵N-N₂O of -79.6‰ vs. air-N₂; minimum δ¹⁸O-N₂O of -4.7‰ vs. Vienna standard mean ocean water), providing new end points for these parameters in natural systems. The extremely depleted nitrogen and oxygen isotopes, together with nitrogen isotopic isomer data for N₂O, imply that most of the N₂O was produced via incomplete nitrification and has undergone virtually no subsequent consumption. However, molecular evidence provides little support for metabolically active nitrifying populations at depths where the maximal N₂O concentrations occur and contemporary biogeochemical reactions cannot explain the extreme excesses of N₂O in Lake Bonney. The gas appears to be a legacy of past biogeochemical conditions within the lake, and in the absence of a significant sink and the presence of a highly stable water column, gradients in N₂O produced by past microbial activity could persist in the cold saline waters of Lake Bonney for >10⁴ years.

¹ Corresponding author (jpriscu@montana.edu).

Acknowledgments

We thank M. T. Downes for numerous discussions, W. Showers for initial isotopic measurements of NO₃⁻, and M. Voytek and J. K. Böhlke for support of K.L.C. in the isotopic analyses of NH₄⁺. The comments by two anonymous reviewers greatly improved the manuscript.

This study was funded by National Science Foundation grants OPP-432595, OPP-0237335, OPP-0440943, and OPP-0631494 awarded to J.C.P. B.C.C. was supported by National Science Foundation grants EAR-0525567 and OPP-0636828. Logistic support was provided by Raytheon Polar Services and Petroleum Helicopters Inc.

This is School of Ocean and Earth Science and Technology contribution 7484.

Lake Bonney, located within the McMurdo Dry Valleys, Antarctica, provides a novel aquatic system to study biogeochemical transformations of water column constituents. The ice cover eliminates wind-induced turbulence, and together with low advective stream input and strong chemical stratification, vertical mixing within the liquid water column is restricted to molecular diffusion (Spigel and Priscu 1998). Under these conditions, geochemical gradients can persist for >50,000 yr (Priscu et al. 1996) and the deep saline waters are estimated to be >10⁵ yr old (Poreda et al. 2004). The lake has two permanently ice-covered lobes (east lobe, ELB; west lobe, WLB) and extensive data sets on the physical, chemical, and biological properties of ELB and WLB from 1990–present have been

compiled as part of the McMurdo Dry Valleys long-term ecological research program (http://www.mcmlter.org/lakes_home.htm).

The seminal work on nitrous oxide (N_2O) in Antarctic lakes was conducted in Lake Vanda (Vincent et al. 1981). Vincent and colleagues measured N_2O levels ranging from 48% above air saturation immediately beneath the ice cover to a maximum of >20,000% above air saturation in the saline bottom waters. The highest levels of N_2O corresponded to zones of high nitrification potential and a paucity of denitrification, leading these authors to conclude that nitrification was the source for this gas. The high levels of N_2O reported for Lake Vanda prompted subsequent studies of the sources and sinks of this gas in other lakes within the McMurdo Dry Valleys. In the present study, we utilize a multifaceted isotopic and genomic approach to study nitrogen transformations in ELB, with an emphasis on those factors affecting N_2O distributions.

A mid-water N_2O concentration maximum in ELB reaches more than 700,000% saturation relative to the N_2O mixing ratio in air (Priscu et al. 1996; Priscu 1997). As in the study of Lake Vanda by Vincent et al. (1981), the origin of the N_2O in ELB was originally proposed to be the result of microbial nitrification (Priscu et al. 1996; Voytek et al. 1998), though this contention has remained equivocal (Priscu 1997). Nitrifying bacteria (i.e., ammonium-oxidizing bacteria, AOB) produce N_2O as a by-product of their chemolithoautotrophic metabolism, particularly under low but nonzero oxygen conditions (Goreau et al. 1980). Under anaerobic conditions, N_2O may be formed as an intermediate in the process of respiratory denitrification, but can also be consumed via reduction to N_2 by this microbial process. Priscu (1997) showed a correlation between the N_2O concentration and apparent oxygen utilization in ELB, leading him to contend that AOB are the primary source of N_2O (Priscu 1997). Although certain archaea are also known to be nitrifiers (Könneke et al. 2005), archaeal abundance is extremely low in ELB (Glatz et al. 2006; Lanoil and Priscu unpubl. data) and we presume that they play an insignificant role in N_2O transformations within ELB. Despite the geochemical evidence implicating nitrification by AOB as a primary source for N_2O in this lake, deoxyribonucleic acid (DNA) sequence analysis of nitrifier DNA (i.e., 16S ribosomal ribonucleic acid [rRNA] and ammonia mono-oxygenase genes) has suggested that these bacteria decline rapidly in abundance with depth through the chemocline (Voytek et al. 1998), and $^{14}\text{CO}_2$ -based nitrification rate measurements have failed to detect NH_4^+ oxidation at the depth of maximum N_2O concentration (Priscu et al. 1996). Other studies have shown that little microbial activity of any kind occurs in the deep brine of ELB despite the presence of viable cells (Priscu 1997; Ward and Priscu 1997). This lack of microbial metabolism may be the result of metal toxicity associated with the deep brine (Ward et al. 2003, 2005) or thermodynamic constraints that have evolved over time (Lee et al. 2004). In the absence of modern activity consistent with the observed N_2O depth distribution, it has been suggested that the extreme N_2O supersaturation in ELB may be a biogeochemical relict from past microbial activity that was present during the

climate-driven evolution of the lake (Priscu et al. 1996; Priscu 1997). Clearly, the sources and sinks of the extreme levels of N_2O in ELB remain unresolved.

We addressed the biogeochemistry of N_2O in ELB using the nitrogen stable isotopic composition ($\delta^{15}\text{N}$) of NH_4^+ , NO_3^- (plus NO_2^-), and N_2O ; the oxygen stable isotopic composition ($\delta^{18}\text{O}$) of N_2O and of H_2O ; and the differential values for $\delta^{15}\text{N}$ within the linear NNO molecule (i.e., N_2O isotopic isomer [isotopomer] analysis) with depth. Parallel molecular biological analyses were conducted to identify the depths where there was active expression of the 16S rRNA genes from all bacteria and specific groups of nitrifying bacteria. We analyze our new data in the context of Lake Bonney's evolutionary history to evaluate the working hypothesis that the N_2O anomaly in ELB is a biogeochemical legacy.

Methods

Site description—Lake Bonney is located within the McMurdo Dry Valleys, Antarctica ($77^\circ 00'\text{S}$, $162^\circ 52'\text{E}$) and is one of several lakes in the region with year-round liquid water and a permanent ice cover. This area is the largest ice-free expanse on the Antarctic continent ($\sim 4000\text{ km}^2$) with a mean annual air temperature of $\sim -20^\circ\text{C}$ and low annual precipitation of $< 10\text{ cm yr}^{-1}$ (Doran et al. 2002). Lake Bonney is in a hydrologically closed basin that is fed by glacial melt for ~ 6 weeks each year during the austral summer and is completely without sunlight from mid-April to mid-August. The ELB (3.8 km^2) and WLB (2.1 km^2) of Lake Bonney are $\sim 40\text{ m}$ deep, covered by 4–5 m of ice, and chemically stratified, with hypersaline ($\sim 3\text{--}5\times$ seawater) and suboxic deep waters (Spigel and Priscu 1996, 1998). ELB and WLB are separated by a bedrock sill at $\sim 13\text{ m}$, which allows relatively fresh surface waters from WLB to flow into ELB, but prevents direct exchange of the deep saline waters between the two basins (Spigel and Priscu 1998), which leads to biogeochemically distinct deep water systems (Priscu et al. 1996; Priscu 1997).

Limnological field collections—Water samples were collected through a $\sim 25\text{-cm}$ -diameter hole in the ice cover at a central position over the deepest waters in ELB. Hydrocasts for temperature, conductivity, dissolved oxygen, nutrients, and other routine limnological data were collected as described previously (Priscu 1995; Priscu et al. 1996; see also www.mcmlter.org/queries/lakes/lakes_home.jsp). Water for N_2O measurements was collected with a 5-liter Niskin bottle and transferred with silicone tubing to clean 125-mL borosilicate serum bottles. To avoid mixing with the atmosphere, the silicone tubing was placed in the bottom of the bottles and $\sim 500\text{ mL}$ of sample was allowed to purge the bottles before final collection. The bottles were sealed with butyl rubber stoppers and aluminum crimp seals such that no headspace remained. Gas concentrations were determined within 5 h at a field site laboratory using a Perkin Elmer 8000 gas chromatograph equipped with an electron capture detector after multiple equilibrations in a 10-mL glass syringe as outlined by Priscu et al. (1996). Parallel samples for isotopic analysis were collected as

above and stored in the dark at 4°C. The isotopic analyses were conducted within 6 months after sample collection. A separate set of experiments (data not shown) confirmed that no significant changes in dissolved N₂O concentration or isotopic ratios occurred during 12-month storage under these conditions.

Samples (1 liter) for RNA extraction were concentrated onto 90-mm 0.2- μ m Durapore polyvinylidene fluoride membrane filters (Millipore) at \sim 5°C using a vacuum of 25 kPa. The filters were then incubated with 5 mL of RNeasy (Ambion) for 5 min. After this incubation, all liquid was removed from the filters by applying vacuum (25 kPa). The filters were then placed in a cryogenic vial containing 2 mL of RNeasy and frozen in liquid N₂ for transport to McMurdo Station, where they were stored at -80°C for shipment to Montana State University, Bozeman for processing (<3 months after collection).

The depths of sample collection are measured from the level of the water in the sampling hole drilled through the ice (i.e., piezometric depth). The lake level (hence the piezometric depth of any persistent chemical feature) varies interannually because of variations in seasonal freshwater input from streams to the layer immediately below the ice cover. Because our samples were collected over several austral summer field seasons (October–January) between 1994 and 2005, a period where the lake level varied by more than 3 m, all data are normalized to the depth measurements of 1994 by alignment of the water column profiles to the chemocline depth as described by Spigel and Priscu (1998). Hence, all depths presented herein are references to the water level within the sampling hole, adjusted to the lake elevation present in 1994.

Isotopic analyses of N₂O, NO₃⁻, and NH₄⁺—The stable isotopic composition of dissolved N₂O was measured by isotope ratio monitoring mass spectrometry using either a Finnigan MAT 252 or Finnigan DeltaPlus instrument. For bulk $\delta^{15}\text{N}$ and $\delta^{18}\text{O}$ measurements, the N₂O was stripped from solution with a helium carrier, concentrated by cryofocusing, and purified by capillary gas chromatography before introduction to the mass spectrometer. Details of the analytical system are described in Dore et al. (1998). For samples with elevated N₂O concentrations, an aliquot of water was injected with a gas-tight syringe into a helium-purged serum vial and the headspace was subsequently analyzed. Following international convention, we report isotopic values in delta notation as per mil (‰) vs. air N₂ for nitrogen and ‰ vs. Vienna standard mean ocean water for oxygen. Our primary standard gas cylinder was isotopically characterized as described in Dore et al. (1998) and Westley et al. (2007). The analytical reproducibility for this method was $\pm 0.2\text{‰}$ and $\pm 0.5\text{‰}$, or better, for $\delta^{15}\text{N}$ and $\delta^{18}\text{O}$, respectively.

We also characterized the position-dependent $\delta^{15}\text{N}$ of the nitrogen atoms within the linear NNO molecule (isotopomer analysis) following the method of Toyoda and Yoshida (1999). This was accomplished by monitoring both the molecular N₂O⁺ and the fragment NO⁺ ions using the DeltaPlus instrument, which can simultaneously measure ions of mass-to-charge ratios 44, 45, 46, 30, and 31.

Following the convention of Toyoda and Yoshida (1999), we refer to the ^{15}N enrichment of the N atoms in the central and end positions of N₂O as $\delta^{15}\text{N}^{\alpha}$ and $\delta^{15}\text{N}^{\beta}$, respectively. The site preference (SP) for ^{15}N enrichment is calculated as: $\text{SP} = \delta^{15}\text{N}^{\alpha} - \delta^{15}\text{N}^{\beta}$. Bulk $\delta^{15}\text{N}$ and $\delta^{18}\text{O}$ data are also available from these measurements. Although the absolute calibration of $\delta^{15}\text{N}^{\alpha}$ and $\delta^{15}\text{N}^{\beta}$ has been a matter of debate, we have accepted the calibration method of Toyoda and Yoshida (1999), on the basis of the recommendations of Westley et al. (2007). This method involves the synthesis of an N₂O standard from the thermal decomposition of NH₄NO₃, which has undergone independent analyses of the NH₄⁺ and NO₃⁻ nitrogens following chemical separation. A cross-calibration exercise with S. Toyoda of the Tokyo Institute of Technology confirmed our results within experimental error (Westley et al. 2007). The reproducibility of our N₂O isotopomer analyses was $\pm 0.9\text{‰}$ for $\delta^{15}\text{N}^{\alpha}$ and $\pm 1.5\text{‰}$ for $\delta^{15}\text{N}^{\beta}$.

The nitrogen stable isotopic composition of dissolved NO₃⁻ (plus NO₂⁻) was determined using the denitrifier method (Sigman et al. 2001). In this method, a bacterial denitrifier that lacks nitrous oxide reductase activity (*Pseudomonas chlororaphis*; ATCC no. 43928) is used to quantitatively convert NO₃⁻ and NO₂⁻ to N₂O for mass spectrometric analysis. The product N₂O was extracted and analyzed for bulk $\delta^{15}\text{N}$ as described above. Standardization was achieved using a previously characterized pure N₂O gas cylinder (described above) and validated using the internationally recognized KNO₃ reference material IAEA-N3 ($\delta^{15}\text{N} = 4.7\text{‰}$). Analytical reproducibility for nitrate $\delta^{15}\text{N}$ was $\pm 0.2\text{‰}$ or better. Because of the large oxygen isotope exchange with water exhibited during denitrification by *P. chlororaphis* (Casciotti et al. 2002), we were not able to obtain $\delta^{18}\text{O}$ values for NO₃⁻ in these samples.

Nitrogen isotopic analyses of dissolved NH₄⁺ were made using an NH₃ diffusion method (Holmes et al. 1998). This method converts NH₄⁺ to NH₃ under basic conditions with subsequent trapping of the liberated gas onto an acidified glass fiber filter. The filter is subsequently combusted and the combustion products reduced to yield N₂ for introduction to the mass spectrometer. Diffusion packets were made by adding 25 μL of 2 mol L⁻¹ H₂SO₄ to ashed 10 mm GF/D filters that were “sandwiched” between two 25-mm Teflon filters. Water samples for NH₄⁺ isotope analysis were aliquoted into replicate acid-washed 125-mL or 250-mL polyethylene bottles in volumes (20–150 mL) adjusted to achieve approximately 4 μmol of N as NH₄⁺ per analysis. Deionized water (DIW) was added to adjust the salinity of each water sample to approximately 35. Ammonium sulfate reference materials USGS-N5 ($\delta^{15}\text{N} = -30\text{‰}$) and USGS-N8 ($\delta^{15}\text{N} = 0.5\text{‰}$) were also prepared by dissolving these materials (2, 3, and 4 μmol each) in 100 mL of DIW. Baked NaCl (650°C for 2 h) was added to NH₄⁺ reference solutions and DIW blanks to raise the salinity to 35 for consistent diffusion recoveries. Prepared diffusion packets were placed in each diffusion bottle, then \sim 1 g of baked MgO was added to each bottle to buffer the pH at \sim 9.7 and the lids tightened. Samples were allowed to diffuse by incubating at 37°C for 5–7 d with gentle shaking. At the end of each incubation period,

the diffusion packet was removed from the sample bottle and placed in an open glass scintillation vial to dry in a H₂SO₄-charged desiccator for 2 d. After the drying period, the lids were placed tightly on the individual scintillation vials for storage. After all diffusion packets were collected and dried, the packets were opened and the 10-mm GF/D filters were packed in tin capsules and analyzed via online combustion using a Carlo Erba elemental analyzer connected to a Finnigan DeltaPlus mass spectrometer through a ConFlo interface. In addition to the reference materials that underwent the diffusion process, the reference materials USGS-N5 and USGS-N8 were weighed directly into replicate tin capsules to test for diffusion recovery and size dependence. Filter blanks and tin capsule blanks were also analyzed as controls. Diffusion recoveries were assessed by comparing N₂ yields to expected peak areas on the basis of NH₄⁺ concentrations and volumes analyzed of the original samples; sample recoveries were all greater than 85%. $\delta^{15}\text{N}$ corrections were then performed on the basis of reference material recoveries and the relation given by Holmes et al. (1998) for fractionation from incomplete recovery. These corrections to the $\delta^{15}\text{N}$ were less than 3‰ in all cases.

Molecular biological analyses—Total RNA was isolated from the filtered cells using the RNeasy mini kit (Qiagen). The initial steps of the protocol recommended by the manufacturer were modified to accommodate isolations from filter-concentrated cells. Clean stainless steel forceps and scissors (baked at 550°C for 12 h) were used to cut the filter into small pieces within a clean petri dish. The filter pieces were equally divided between four 2-mL bead-beating tubes that were 20% full of 0.1-mm zirconium beads (Biospec Products) and contained 600 μL of guanidine salt buffer provided by the manufacturer (RLT™; Qiagen). Cells were lysed using a FastPrep FP120 bead-beater apparatus (Savant) for 45 s at setting 6.5, and the tubes were then immediately placed on ice. The extraction tubes were centrifuged for 10 min at 15,000 $\times g$ at 4°C and the supernatant (~550 μL) was transferred to a clean microcentrifuge tube. Each tube was washed with 300 μL of RLT buffer, centrifuged, and the supernatants pooled (total recovery of ~850 μL). An equal volume of 70% ethanol (850 μL) was added to each sample (4 \times 1700 μL), and 700 μL of the mixture was added to a RNeasy minicolumn and centrifuged for 15 s at 8000 $\times g$. The effluent from the RNeasy minicolumn was removed, another 700 μL of sample was added to the column, and the process was repeated until the entire sample (6.8 mL) had passed through the column. From this point on, the protocol recommended by the manufacturer (Qiagen) was followed precisely.

Contaminating DNA was digested by incubating 5 μL of the eluted nucleic acid pool with 1 unit of RQ1 RNase-free DNase (Promega) for 30 min at 37°C. The enzyme was inactivated by the addition of 1 μL of RQ1 DNase STOP, followed by incubation at 65°C for 10 min. First-strand cDNA was synthesized using the SuperScript™ II RNase H⁻reverse transcriptase (Invitrogen). Seven microliters of DNased RNA was combined with 1 μL (2 pmol) of the 16S

rRNA gene primer 1391R (Lane 1991) and 1 μL of mixed deoxyribonucleotide triphosphates (10 mmol L⁻¹ each), followed by incubation at 65°C for 5 min. The tubes were cooled on ice for at least 1 min. To this mixture, 4 μL of 5 \times buffer (Invitrogen), 2 μL of 0.1 mol L⁻¹ dithiothreitol, and 1 μL of RNasin (Promega) were added and incubated at 42°C for 2 min. Second-strand synthesis was initiated with the addition of 1 μL (200 units) of SuperScript™ II, followed by incubation at 42°C for 50 min. Samples were incubated at 70°C for 15 min to inactivate the SuperScript™ II enzyme.

One microliter of cDNA was used as the template for 30 cycles of polymerase chain reaction (PCR) amplification (Eppendorf MasterTaq Kit) in an Eppendorf Mastercycler gradient thermal cycler using a 50°C annealing temperature, a final MgCl₂ concentration of 1.5 mmol L⁻¹, and 5 pmol of the universal 16S rRNA gene primers 27F and 1391R (Lane 1991). A nested PCR was then performed with 1 μL of the product from the latter reaction and the same amplification conditions as above, except using the 16S rRNA nucleotide primers specific for nitrifying β - (Voytek and Ward 1995) and γ -proteobacteria (Freitag and Prosser 2003) at an annealing temperature of 58°C. Samples treated with DNase that were not reverse transcribed served as controls to monitor for potential genomic DNA contamination of the cDNA. All reactions were evaluated by electrophoresis through a 1% agarose gel followed by staining with ethidium bromide.

Individual cDNA molecules from the ~1100-base-pair populations were cloned into the pGEM-Teasy vector (Promega) and 40 clones with inserts of the predicted size were screened for sequence diversity by restriction fragment length polymorphism with the restriction enzymes *Hin*PI and *Msp*I (New England Biolabs). Clones with unique inserts were bidirectionally sequenced using primers that annealed the flanking T7 and SP6 universal promoter sequences. The amplified sequences were checked for chimeras using the Ribosomal Database Project II Chimera Check (<http://rdp.cme.msu.edu/>) and Bellerophon Server (<http://foo.maths.uq.edu.au/~huber/bellerophon.pl>), manually evaluated for covariance, and aligned on the basis of positional homology for phylogenetic analysis using the ARB software package (<http://www.arb-home.de/>) and the beta-4b10 version of PAUP 4.0 (Sinauer Associates).

Results

Physicochemical properties—Temperature and conductivity profiles in ELB were similar to those measured previously, owing to the extraordinary stability of the water column (Spigel and Priscu 1998). Temperatures reached a mid-depth maximum of 6°C and fell below 0°C in the deep-water brine (Fig. 1A). The conductivity data reveal the high level of vertical stratification with freshwater overlying a layer of hypersaline water (~11 S m⁻¹) with a chemocline between 15 and 20 m. Dissolved oxygen levels in ELB ranged from highly supersaturated (>295% of air saturation) above the chemocline transitioning to suboxic conditions (<7% of air saturation) below 25 m (Fig. 1A). Dissolved inorganic nitrogen compounds increased rapidly with depth through the chemocline, reaching deep-water

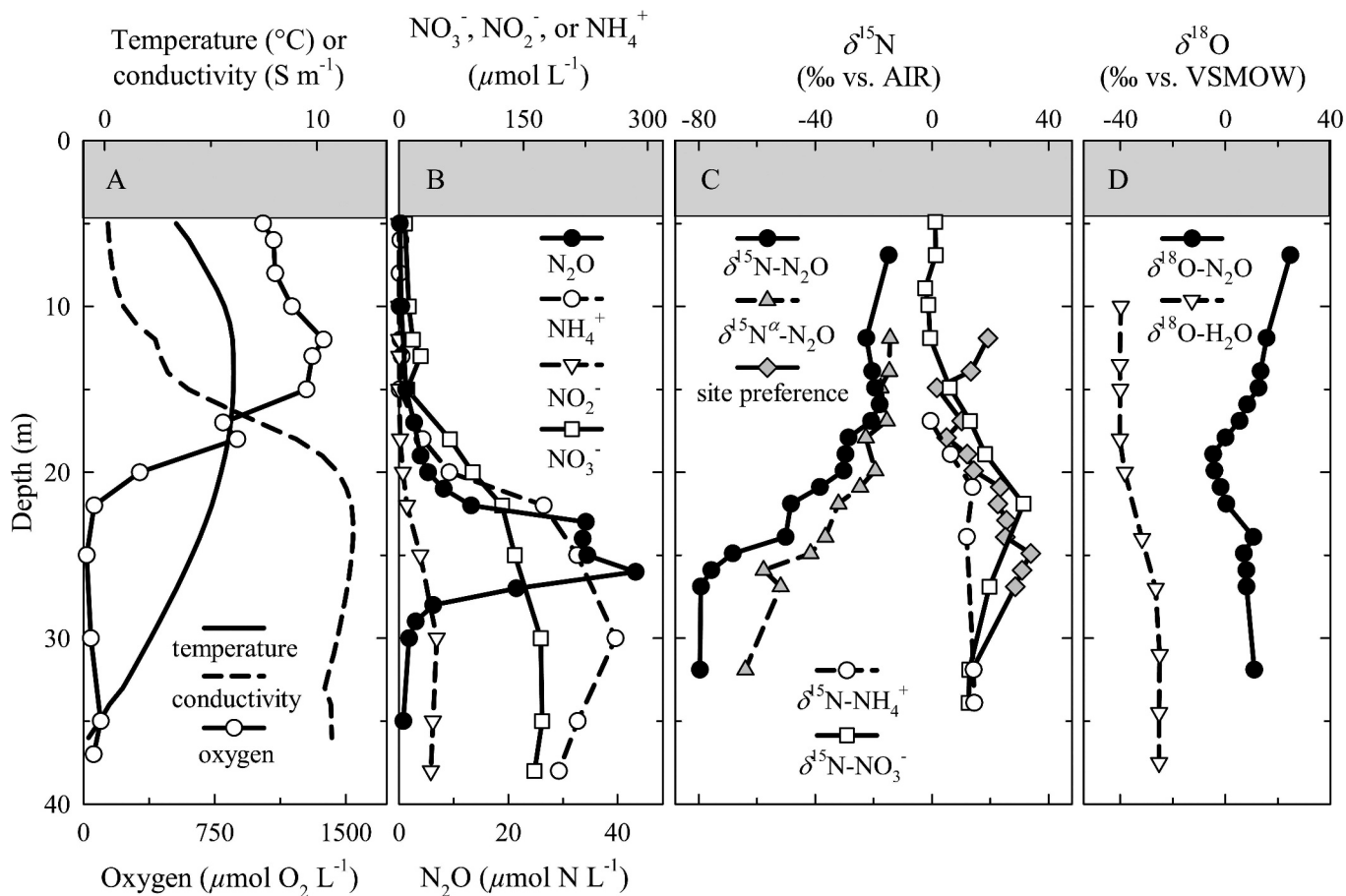


Fig. 1. Profiles of (A) temperature, salinity, and oxygen concentration; (B) NH_4^+ , NO_3^- , NO_2^- , and N_2O concentrations; (C) $\delta^{15}\text{N}$ values for N_2O ($\delta^{15}\text{N}\text{-N}_2\text{O}$, $\delta^{15}\text{N}\alpha\text{-N}_2\text{O}$, and site preference), NO_3^- , and NH_4^+ ; and (D) the $\delta^{18}\text{O}$ values of N_2O and H_2O vs. depth in ELB. Depths are normalized to the 1994 lake elevation (see Methods). $\delta^{18}\text{O}\text{-H}_2\text{O}$ values are from Matsubaya et al. (1979). The gray shading in the upper 5 m demarcates ELB's permanent ice cover.

maxima of 173, 45, and 261 $\mu\text{mol L}^{-1}$ for NO_3^- , NO_2^- , and NH_4^+ , respectively (Fig. 1B). Dissolved N_2O concentrations varied by more than two orders of magnitude with depth. Above 15 m and below 30 m, N_2O was relatively low ($<1 \mu\text{mol N L}^{-1}$), with the highest concentration (43.3 $\mu\text{mol N L}^{-1}$) occurring at 26 m (Fig. 1B).

Stable isotopes—The $\delta^{15}\text{N}$ values of NH_4^+ were relatively constant ($\sim 14\%$) in the water below 20 m, with $\delta^{15}\text{N}\text{-NH}_4^+$ dropping to near 0‰ by 17 m (Fig. 1C). Owing to the relatively low NH_4^+ concentrations above 17 m, large sample sizes are needed for the NH_4^+ isotopic analyses, and consequently, no data were collected above 17 m.

The nitrogen isotopic composition of dissolved NO_3^- (plus NO_2^-) was similar to that of NH_4^+ in the deep water, and was near the $\delta^{15}\text{N}$ value of atmospheric N_2 at depths above 15 m (Fig. 1C). At intermediate depths, NO_3^- was enriched in ^{15}N relative to NO_2^- at shallower depths, with a peak $\delta^{15}\text{N}$ value of 31.4‰ at 22 m. This enrichment suggests a local sink of low $\delta^{15}\text{N}\text{-NO}_3^-$, possibly through dissimilatory NO_3^- reduction to NH_4^+ . $\delta^{15}\text{N}\text{-NO}_3^-$ values decreased from 31.4‰ to 19.7‰ through the zone of highest N_2O concentrations (22–27 m) then decreased further to $\sim 12.7\%$ just above the bottom of the lake.

The bulk ^{15}N content of N_2O was substantially depleted in the deep brine, reaching a minimum $\delta^{15}\text{N}$ value of -79.6% at 32 m (Fig. 1C). From 32 m up to the N_2O maximum at 26 m, $\delta^{15}\text{N}\text{-N}_2\text{O}$ values were relatively constant, then increased rapidly to -50.2% at 24 m, followed by a more gradual increase to -14.9% from 24 m up to 7 m. Isotopomer analyses revealed that $\delta^{15}\text{N}\alpha\text{-N}_2\text{O}$ values were also low in the deep waters, but to a lesser extent than the bulk $\delta^{15}\text{N}\text{-N}_2\text{O}$ values (Fig. 1C). Consequently, the site preference for ^{15}N enrichment in N_2O was positive. The maximum SP was 33.9‰ at 25 m, within the N_2O maximum layer. From 25 m downward to 32 m the SP decreased to 13.8‰, whereas it decreased from 25 m upward to a minimum value of 1.7‰ at 15 m (Fig. 1C). Above this upper minimum, SP rose to 19.2‰ at 12 m; isotopomer data were not collected at shallower depths. The oxygen stable isotopic composition of N_2O was relatively constant within and below the N_2O maximum layer, with $\delta^{18}\text{O}$ values of $\sim 7\text{--}11\%$ (Fig. 1D). From 17 to 24 m, there was a pronounced minimum in $\delta^{18}\text{O}\text{-N}_2\text{O}$ values, reaching a low at 19 m of -4.7% . From this minimum upward, the $\delta^{18}\text{O}\text{-N}_2\text{O}$ values rose to a high of 24.8‰ at 7 m. The $\delta^{18}\text{O}\text{-N}_2\text{O}$ values are compared with historical measurements of $\delta^{18}\text{O}$ in ELB water (Matsubaya et al. 1979) in Fig. 1D. Low $\delta^{18}\text{O}\text{-H}_2\text{O}$

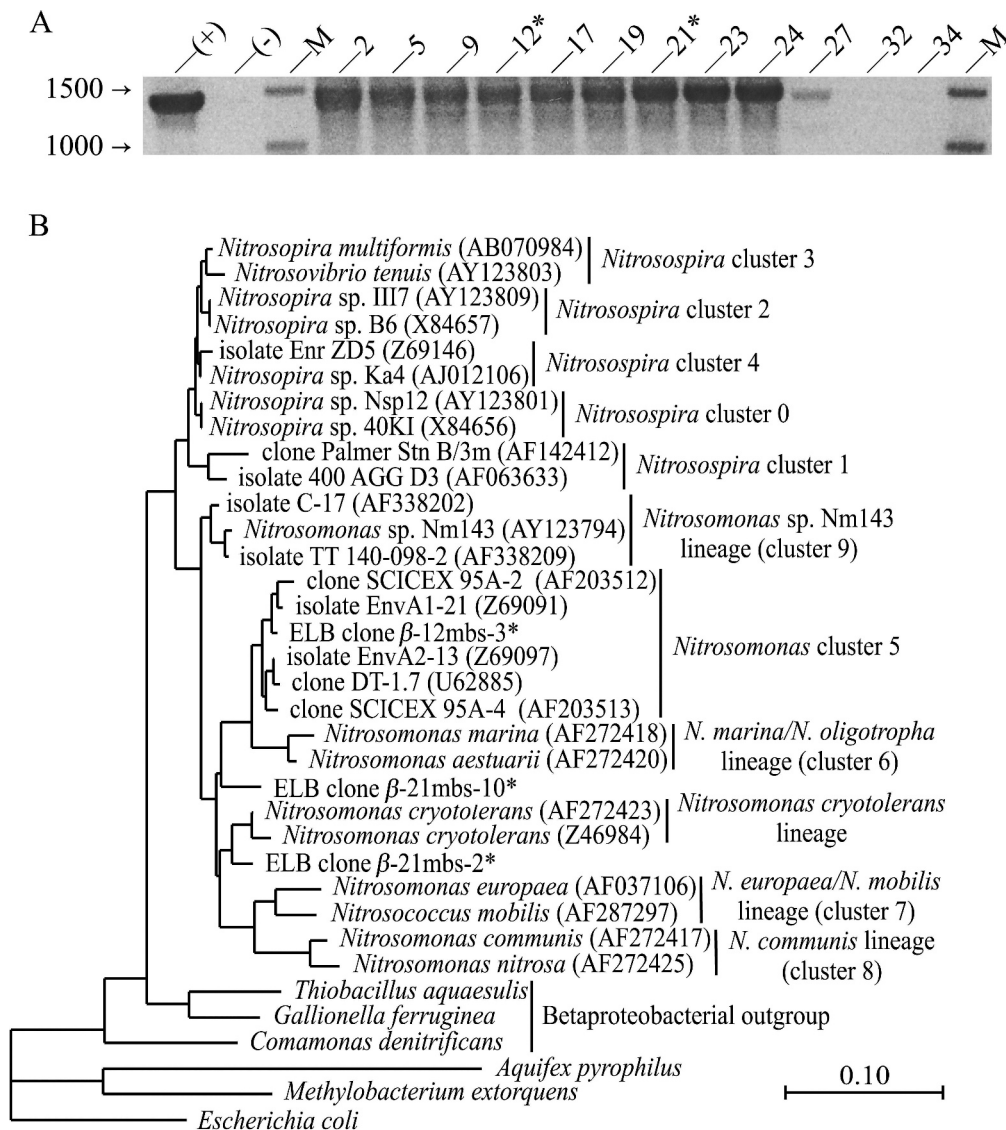


Fig. 2. (A) RT-PCR-amplified small-subunit rRNA molecules from ELB, analyzed by agarose gel electrophoresis and staining (negative image shown). Amplification was conducted using the “universal” oligonucleotide primers 27F and 1391R (Lane 1991). Positive (+) and negative (-) controls and the molecular weight marker (M) are indicated. The amplified populations from depths 12 and 21 m (asterisks) were subsequently used as template for the sequences generated (panel B), as described in the text. (B) Phylogenetic analysis of RT-PCR 16S rRNA sequences from ELB related to β -proteobacterial AOB. The sequences obtained (marked with asterisks), corresponding to nucleotides 181 to 1204 of the *Escherichia coli* 16S rRNA gene, were aligned on the basis of secondary structure. The maximum likelihood tree was generated using a 1024-nucleotide mask of unambiguously aligned positions. GenBank accession numbers are listed in parentheses. Relatives from the known clusters of β -proteobacterial AOB are included (Freitag and Prosser 2004). The scale bar indicates 0.1 fixed substitutions per nucleotide position.

values (about -40%) typical of modern Antarctic meteoric water were measured in the shallow freshwaters, whereas relatively higher $\delta^{18}\text{O}\text{-H}_2\text{O}$ values (about -25%) were observed in the deep brine.

Detection of rRNA from NH_4^+ -oxidizing bacteria—Small-subunit rRNA molecules were amplified using reverse-transcription PCR (RT-PCR) and a set of “universal” oligonucleotide primers from all depths above 27 m, but were not detected in samples collected from 32 and 34 m (Fig. 2A). Using the RT-PCR-amplified DNA populations as a template, nested amplifications were

conducted using primers designed to target β -proteobacterial AOB 16S rRNA sequences (Voytek and Ward 1995), yielding DNA product of the predicted size (~ 1.1 kb) for all depths above 21 m. No amplification occurred in any of the samples analyzed using primers that target γ -proteobacterial AOB 16S rRNA gene sequences (Freitag and Prosser 2003).

Discussion

Isotopic constraints on N_2O sources and sinks—There are several microbially mediated processes that can transform

N₂O in aquatic systems, and each of these processes has kinetic isotopic fractionation associated with it. The measured abundance of the rare isotopes (¹⁵N, ¹⁸O) relative to the common isotopes (¹⁴N, ¹⁶O) in N₂O represents the combined effects of all processes affecting N₂O production and consumption, the degree to which these reactions have progressed, and the original isotopic compositions of the source reactants. We may therefore use our isotopic measurements to constrain the microbial processes that have influenced N₂O concentrations in ELB.

The two most important biological processes influencing N₂O concentration are nitrification and denitrification (Stein and Yung 2003). The production of N₂O via classical nitrification is carried out by aerobic chemolithoautotrophic bacteria (and archaea) that obtain energy from the oxidation of NH₄⁺ to NO₂⁻ via the intermediates NH₂OH and NO. A small fraction of these intermediates may be converted to N₂O as a by-product rather than being completely converted to NO₂⁻ (Ostrom et al. 2000; Wrage et al. 2001). In addition, under suboxic conditions AOB may reduce to N₂O a fraction of the NO₂⁻ that they generate in a process known as nitrifier denitrification (Wrage et al. 2001). The yield of N₂O from AOB is enhanced under reduced oxygen levels, although the mechanism is not well understood (Goreau et al. 1980). Heterotrophic nitrification by chemo-organotrophic bacteria and fungi can also produce N₂O via reduction of the NO₂⁻ resulting from NH₄⁺ oxidation, but this aerobic process is probably ecologically most important in acidic soils with a high carbon load (Stein and Yung 2003; Revsbech et al. 2006).

Classical denitrification, in contrast, is an anaerobic process in which NO₃⁻ is used as a terminal electron acceptor in the respiration of organic carbon. The end product of denitrification is N₂, but some fraction of the gaseous intermediate N₂O may escape further reduction and accumulate (Wrage et al. 2001; Stein and Yung 2003). In aquatic environments, nitrification and denitrification often occur in proximity at oxic–anoxic boundaries (Downes 1988; Revsbech et al. 2006). Although other reductive microbial processes have been demonstrated to produce some N₂O, such as NO₂⁻ assimilation by green algae (Weathers 1984) and dissimilatory NO₃⁻ reduction by bacteria (Samuelsson 1985), their quantitative significance to N₂O production in aquatic environments is not well established.

Large kinetic nitrogen isotope effects are associated with NH₄⁺ oxidation to NO₂⁻ (15–35‰) via autotrophic nitrification and with NO₂⁻ reduction to N₂O (15–32‰) via nitrifier denitrification (Yoshida 1988; Casciotti 2002; Casciotti et al. 2003). These isotope effects would be expected to produce N₂O with a δ¹⁵N value that is significantly lower than that of the source NH₄⁺. Yoshida (1988) found in laboratory experiments that N₂O produced by the nitrifier *Nitrosomonas europaea* was depleted in ¹⁵N by up to 63‰ compared with the NH₄⁺ substrate. He attributed these extreme depletions to sequential kinetic isotope effects in the oxidation of NH₄⁺ to NO₂⁻ and the subsequent reduction of NO₂⁻ to N₂O. A large depletion would likewise be expected if N₂O were produced from

sequential oxidation of NH₄⁺ to NH₂OH and NO followed by reduction of the NO intermediate (Naqvi 1991), rather than from reduction of NO₂⁻, but the kinetic isotope effects associated with NO oxidation and reduction are not established (Casciotti et al. 2003).

Denitrification also produces N₂O, which is depleted in ¹⁵N compared with its substrate (NO₃⁻) (Barford et al. 1999). However, N₂O is simultaneously consumed in this process, so the N₂O produced in a denitrification regime with a high degree of simultaneous consumption may become enriched in ¹⁵N (Yoshinari et al. 1997). At steady state, the kinetic isotope effect associated with N₂O reduction to N₂ causes the residual N₂O pool to be enriched in ¹⁵N relative to the product N₂ and leaves the δ¹⁵N-N₂O values typically only ~15‰ depleted compared with the source NO₃⁻ (Barford et al. 1999).

On the basis of the high potential variability in δ¹⁵N-N₂O, it is difficult to attribute microbial sources of N₂O on the basis of δ¹⁵N alone. Oxygen isotopes in N₂O are also affected by kinetic isotope fractionations, but the resulting δ¹⁸O-N₂O signature can be complicated by isotopic exchange with water and by variations in the δ¹⁸O value of molecular oxygen (Ostrom et al. 2000). Importantly, the SP for ¹⁵N enrichment between the central (α) and end (β) positions of N in the NNO molecule that is introduced during N₂O formation is independent of the bulk isotopic composition of the substrate and is distinct between oxidative and reductive microbial processes generating N₂O; for both classical respiratory denitrification and nitrifier denitrification, the SP is ~0‰, whereas for classical nitrification the SP is ~33‰ (Sutka et al. 2006). Reduction of N₂O during denitrification can lead to an increase in the SP of the remaining N₂O pool, but no known removal process can reduce the SP of N₂O (Ostrom et al. 2007). Hence, SP values near 0‰ can only result when N₂O reduction is essentially absent. Moreover, in the absence of N₂O reduction, the SP of N₂O can be used to quantitatively apportion its oxidative and reductive sources (Sutka et al. 2006; Ostrom et al. 2007).

N₂O within the deep water (>25 m) of ELB displays an extremely low nitrogen isotopic value of ~-80‰, which is ~94‰ below that of both the NH₄⁺ and the NO₃⁻ pools (Fig. 1C). The extent of this depletion is greater than anticipated for either nitrification or denitrification. However, no known nitrogen cycle process results in a more extreme ¹⁵N depletion than does nitrification (Yoshida 1988), and kinetic isotope effects associated with nitrification are known to vary between strains of AOB (Casciotti et al. 2003) and possibly with environmental conditions. Importantly, within the N₂O maximum from 25–27 m, the SP of N₂O is 31.1‰ ± 2.7‰ (mean ± SD). Given the extremely low bulk δ¹⁵N-N₂O in this layer, it is unlikely that any significant N₂O reduction has occurred there. Assuming that there has been no reduction of N₂O, the observed SP value implies that 94% ± 8% of the N₂O in this layer was produced by nitrification, probably via the intermediate NH₂OH (Sutka et al. 2006).

If the source of the N₂O peak is from nitrification, the oxygen within N₂O produced via this pathway would be expected to be derived principally from dissolved O₂

(Ostrom et al. 2000). Atmospheric oxygen has a $\delta^{18}\text{O}$ of 23.5‰ (Ostrom et al. 2000); thus it is not surprising that the $\delta^{18}\text{O}\text{-N}_2\text{O}$ values within the N_2O maximum ($\sim 7\text{--}8\%$) are higher than that of the ambient H_2O (-25% ; Fig. 1D). Unfortunately, $\delta^{18}\text{O}\text{-O}_2$ was not measured in ELB, and the low concentration of dissolved O_2 in the suboxic zone of ELB may be isotopically enriched because of its consumption during microbial respiration; hence we cannot further constrain the relative contributions of O_2 and H_2O to N_2O without knowledge of the $\delta^{18}\text{O}\text{-O}_2$ values within the lake.

$\delta^{15}\text{N}\text{-N}_2\text{O}$ values gradually increase from the N_2O peak up to 19 m, but remain $\sim 50\%$ depleted when compared with $\delta^{15}\text{N}\text{-NH}_4^+$ values, whereas the SP of N_2O declines over this depth interval (Fig. 1C). Over the same depth range, $\delta^{18}\text{O}\text{-N}_2\text{O}$ gradually declines to its minimum value of -4.7% at 19 m (Fig. 1D). These observations suggest that an additional, reductive source of N_2O exists at the base of the chemocline at about 19–20 m. Above this zone the isotopic signatures of N_2O increase toward the ice cover (Fig. 1C), suggesting an influence of atmospheric N_2O , which is characterized by $\delta^{15}\text{N} \approx 7\%$, $\delta^{18}\text{O} \approx 44\%$, and SP $\approx 19\%$ (Kim and Craig 1993; Yoshida and Toyoda 2000). An atmospheric source of N_2O most likely results from the seasonal advection immediately beneath the ice cover of low-density atmospherically equilibrated glacial-melt water into the lake (Matsubaya et al. 1979; Spigel and Priscu 1998).

To examine the mixing of the different N_2O sources in more detail, we plotted N_2O concentration against a conservative tracer (conductivity, as a surrogate for salinity) from the depth of the N_2O maximum at 26 m up to near the underside of the ice cover at 5 m (Fig. 3A). Data from below 26 m were not included because conductivity is essentially constant below this depth. The plot shows conservative mixing of three N_2O end members: the deep N_2O maximum, a presumably atmospheric end member beneath the ice, and a third source at 19–20 m. When SP is similarly plotted against conductivity (Fig. 3B), it becomes evident that the deep N_2O end member has an oxidative source signature (high SP) and the 19–20-m source has a strong reductive contribution to its signature (low SP). The mixing line from 19 m to 5 m has a y -intercept of SP = 18.7‰, which is consistent with an atmospheric N_2O end member in the freshwater immediately beneath the ice cover. The very low SP value at 15 m is inconsistent with the conservative mixing indicated by the N_2O concentration data in Fig. 3A; we presume that SP data from this depth represent an analytical artifact and do not include it in our interpretation of mixing processes in the 19 m to 5 m depth interval.

When the bulk nitrogen and oxygen isotopic data from ELB are plotted against each other, further evidence is revealed for mixing of N_2O among three components of differing isotopic signatures (Fig. 4A). The major N_2O isotopic end members are again associated with the N_2O maximum (26 m), a second source at 19–20 m, and a near-surface source. The N_2O within the maximum occurs in a zone of relatively low O_2 concentration, and is characterized by very low $\delta^{18}\text{O}\text{-N}_2\text{O}$. The low $\delta^{18}\text{O}\text{-N}_2\text{O}$ may be due

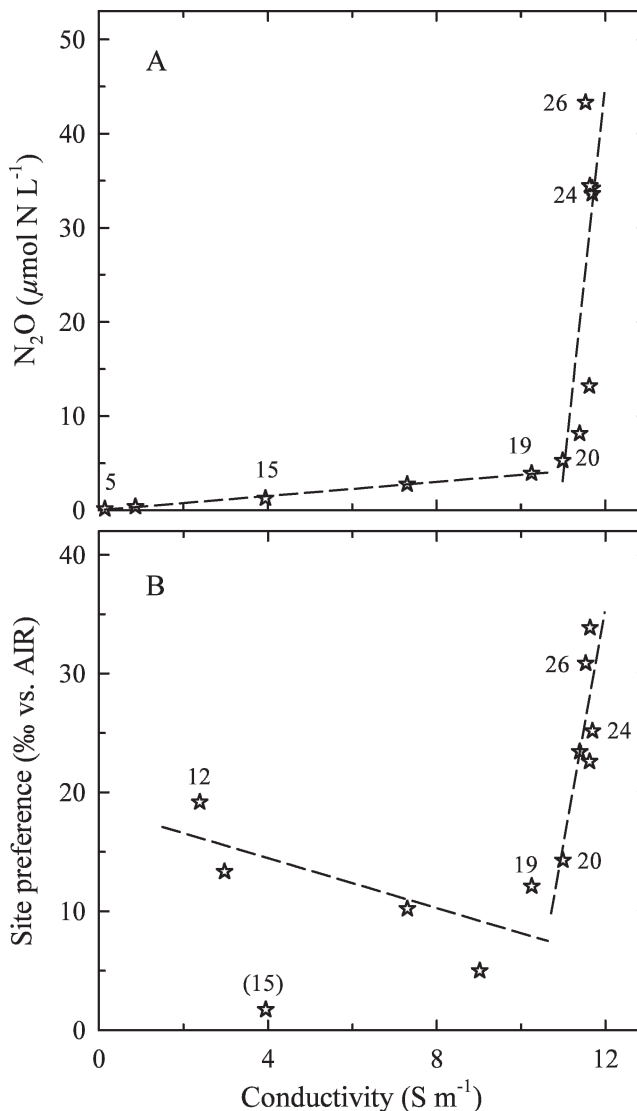


Fig. 3. Cross-plots of (A) N_2O concentration and (B) N_2O nitrogen isotopic site preference vs. conductivity in ELB. Numbers near data points indicate depths of sample collection. Dashed lines represent linear regressions of data from within the 5–19-m layer (immediately beneath the ice cover to the base of the chemocline) and from the 20–26-m layer (base of the chemocline to the N_2O maximum). The 15-m site preference value is considered an outlier possibly resulting from analytical error and was not used in the regression analysis.

to a contribution of oxygen from water, such as would be expected from reduction of NO_2^- during nitrifier denitrification in a low-oxygen setting (Ostrom et al. 2000). The 24-m data point exhibits a high oxygen isotopic value relative to a conservative mixing scenario, which potentially represents an analytical artifact (Fig. 4A). However, the O_2 concentration at 24 m is nearly zero (Fig. 1A) and the N_2O concentration profile exhibits a small inflection at this depth (Fig. 1B); therefore some reduction of N_2O cannot be ruled out entirely. The $\delta^{15}\text{N}$ values of NO_3^- are also high in this layer (Fig. 1C), which could result from nitrate reduction, but owing to the coarse sample spacing for this

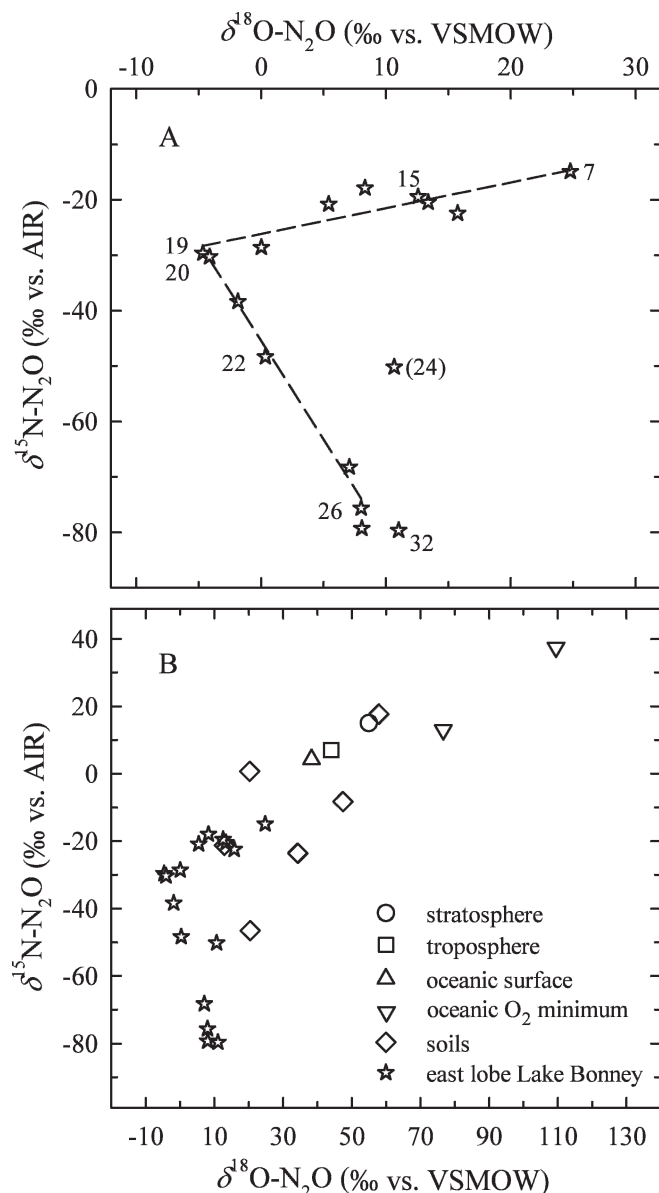


Fig. 4. Cross-plots of $\delta^{18}\text{O}$ vs. $\delta^{15}\text{N}$ of N_2O from ELB and other natural environments. (A) ELB data only. Numbers near data points indicate depths of sample collection. Dashed lines represent linear regressions of data from within the 5–19-m layer (immediately beneath the ice cover to the base of the chemocline) and from the 20–26-m layer (base of the chemocline to the N_2O maximum). The 24-m $\delta^{18}\text{O}$ value is considered an outlier possibly resulting from analytical error and was not used in the regression analysis. (B) ELB data compared with other published values of $\delta^{18}\text{O}$ and $\delta^{15}\text{N}$ of N_2O . Published N_2O isotopic compositions were selected to represent a variety of environments and to demonstrate the full range of previous measurements. The atmospheric data are from Kim and Craig (1993), the oceanic data are from Dore et al. (1998) and Yoshinari et al. (1997), and the soil data are from Bol et al. (2004), Pérez et al. (2001), and Yamulki et al. (2001).

constituent it is impossible to determine whether a maximum in $\delta^{15}\text{N}-\text{NO}_3^-$ values is located precisely at 24 m.

Although the isotopic data reveal likely nitrifier denitrification at depths of 19–20 m, the vast majority of N_2O in

ELB is found in the deep maximum and appears to have been formed via classical nitrification. Deep-water values of $\delta^{15}\text{N}-\text{N}_2\text{O}$ in ELB are lower than any previously reported from natural environments (Fig. 4B), despite relatively modest $\delta^{15}\text{N}$ values for NH_4^+ , the substrate for nitrification. Environmental differences between ELB and other aquatic systems, such as the high NH_4^+ concentration ($\sim 200 \mu\text{mol L}^{-1}$) and salinity (3–5 \times seawater) in the deep water, may lead to greater isotopic fractionation and full expression of kinetic isotope effects involved in nitrification and nitrifier denitrification. Most of the $\delta^{18}\text{O}-\text{N}_2\text{O}$ values in ELB are also lower than any previously reported (Fig. 4B); these depleted oxygen isotopic signatures may be due to both expression of kinetic isotope effects during N_2O production and the influence of highly depleted oxygen from H_2O .

Molecular assessment of NH_4^+ oxidizer activity—A positive correlation between cellular rRNA content and growth rate (DeLong et al. 1989) makes rRNA detection an attractive approach for inferring the metabolically active phylotypes in an environmental sample (Miskin et al. 1999). Ammonia-oxidizing activity has been measured at 12 m using $^{14}\text{CO}_2$ incorporation in the presence and absence of an inhibitor that suppresses NH_4^+ oxidation (Priscu et al. 1996); the clone library constructed at this depth using RT-PCR product from amplifications targeting β -proteobacterial AOB contained one dominant clone that can be confidently assigned within *Nitrosomonas* cluster 5 (Fig. 2B). The two phylotypes identified at 21 m (the deepest depth at which β -proteobacterial AOB clones were detected by RT-PCR) are clearly related to members of the genus *Nitrosomonas*; however, they have a weak phylogenetic association with the marine *Nitrosomonas cryotolerans* lineage (96–97% identity) and cannot be confidently classified within any of the currently recognized β -proteobacterial AOB clusters (Freitag and Prosser 2004). Although RT-PCR products from β -proteobacterial AOB were detected from 2–21 m in ELB, inferences of metabolic activity solely on the basis of the detection of rRNA must be viewed with caution in light of documented reports where cellular rRNA persisted for days in starved, nongrowing cells (Flårdh et al. 1992). It should also be noted that viable but inactive cells also possess a baseline level of ribosomes (Röling and Head 2005) and Wagner et al. (1995) demonstrated that AOB maintain their ribosome content for several hours after cessation of NH_4^+ -oxidizing activity. Despite the potential caveats inherent to data of this nature, the molecular results from ELB (Fig. 2A) corroborate previous work showing that little to no contemporary microbial activity occurs in the deep brine (Priscu 1997; Ward and Priscu 1997), and suggest that activity in *Nitrosomonas*-related lineages is limited to waters above 23 m. This distribution of AOB activity is consistent with in situ measurements of ammonia oxidation made in 1990–1992 using an inhibitor-sensitive ^{14}C technique (Priscu et al. 1996) that revealed a rate maximum at 20 m (≈ 22 m in 1994) and no measurable activity from 22 m (≈ 24 m in 1994) downward. Fluorescent probe in situ hybridization assays have indicated that

there are ~ 500 β -proteobacterial AOB cells mL^{-1} within the N_2O concentration maximum (Voytek et al. 1998); however, multiple lines of evidence imply that the low number of AOB cells present at these depths were not metabolically active when collected for analysis in the current study.

N₂O in ELB: A biogeochemical legacy?—The isotopic data lead us to contend that the deep-water N_2O maximum layer in ELB originated through microbial nitrification, probably via NH_2OH . These results are consistent with the observed high levels of oxidized nitrogen compounds in the nearly anoxic deep water (Fig. 1B), which indicate a lack of bulk denitrifying activity, despite the very low O_2 levels and the presence of viable denitrifying bacteria (Ward and Priscu 1997). The absence of denitrification in the ELB brine may result from high concentrations of growth inhibitors such as toxic metals (Ward et al. 2005), or because of thermodynamic constraints that have evolved over time as climate variations changed the size and ice conditions of the lake (Lee et al. 2004). Our rRNA results imply that metabolically active nitrifying bacteria exist only at depths above 23 m in the ELB water column. How then did the extreme supersaturation layer of nitrification-derived N_2O from 22 to 27 m develop?

Clearly, the biogeochemical gradients in ELB cannot be fully explained without considering the climatic history of the region, and in particular the limnetic evolution of Lake Bonney (Priscu 1995). He isotope ratios and He, Ne, Ar, and N_2 concentrations within the water column of Lake Bonney indicate that WLB has retained an ice cover for $>10^6$ yr, whereas complete ice coverage has only existed on ELB for 200 ± 50 yr (Poreda et al. 2004). Drier and cooler climatic conditions 3000 yr before present (BP) resulted in lowered lake levels in the McMurdo Dry Valleys (Lyons et al. 1998a), which separated WLB and ELB into two disconnected lakes. Evidence from $\delta^{18}\text{O}\text{-H}_2\text{O}$, δD , and $\delta^{37}\text{Cl}$ values imply that these cooler conditions transformed ELB into an ice-free hypersaline lake (Lyons et al. 1998b, 1999). In this scenario, desiccation of the prior lake concentrated its inorganic nutrients and increased the salinity such that only extreme halophiles could tolerate the environmental conditions.

From 3000 to 200 yr BP, rising temperatures would have generated an increased influx of melt water from the nearby glaciers, raising the level of WLB above the sill depth, allowing freshwater to flow from WLB to ELB (Poreda et al. 2004). Assuming the freshwater input from WLB mixed very little with the dense brine layer in ELB, an assumption supported in recent observations of inflow into Lake Bonney during unusually warm years (Foreman et al. 2004), a surface freshwater lens would be formed that would seasonally freeze and thaw. The shallow freshwater layer would be exposed to both a high diffusive flux of nutrients from the brine below and to ample summer light from above, providing eutrophic conditions that would support the rapid growth of phytoplankton and associated microbial communities. Lee et al. (2004) suggest that ELB was more reducing in the past (Eh $\sim 100\text{--}200$ meV compared with a contemporary value of 500 meV) and

predicted that NH_4^+ formation (via dissimilatory NO_3^- reduction) was favorable at depths within the current N_2O concentration maximum; this NH_4^+ formation process could explain why $\delta^{15}\text{N}\text{-NO}_3^-$ is higher than $\delta^{15}\text{N}\text{-NH}_4^+$ in the deep water. High concentrations of NH_4^+ would enhance N_2O production via incomplete nitrification (e.g., $\text{NH}_4^+ \rightarrow \text{NH}_2\text{OH} \rightarrow \text{N}_2\text{O}$; Goreau et al. 1980), while O_2 levels would decline because of microbial respiration. As the depth of the freshwater lens increased, the ice cover eventually became permanent, trapping dissolved gases (Poreda et al. 2004). Because of ELB's unusually stable water column (Spigel and Priscu 1998) and the absence of bulk denitrification, the N_2O gradients produced in such a scenario could persist for time frames $>50,000$ yr (Priscu et al. 1996). Although the $\delta^{15}\text{N}$ and $\delta^{18}\text{O}$ values of N_2O in the bottom water below the concentration maximum are similar to those of N_2O within the maximum, the sample at 32 m has a lower SP; this peculiarity may result from some small amount of N_2O that was already dissolved in the brine at the time the ice cover became permanent, or it could be an analytical artifact.

The isotopic and isotopomeric data confirm that the elevated N_2O in the deep brine of ELB is of microbial origin and are consistent with production via nitrification. Our data, in concert with previously published results, indicate that the N_2O in ELB's concentration maximum cannot be explained by contemporary biogeochemical activity or from glacially derived stream flow, indicating that the N_2O was produced during an earlier evolutionary phase of the lake. Predicted historical conditions 200 yr BP in ELB are compatible with an ecological setting in which large quantities of N_2O could have been produced by incomplete nitrification, forming a distinct concentration maximum. Our results also suggest that some N_2O is presently being formed, likely via nitrifier denitrification, at 19–20 m, well above the relict N_2O peak.

References

- BARFORD, C. C., J. P. MONTROYA, M. A. ALTABET, AND R. MITCHELL. 1999. Steady-state nitrogen isotope effects of N_2 and N_2O production in *Paracoccus denitrificans*. *Appl. Environ. Microbiol.* **65**: 989–994.
- BOL, R., T. RÖCKMANN, M. BLACKWELL, AND S. YAMULKI. 2004. Influence of flooding on $\delta^{15}\text{N}$, $\delta^{18}\text{O}$, ^{15}N and $^{28}\text{N}_2$ signatures of N_2O released from estuarine soils—a laboratory experiment using tidal flooding chambers. *Rapid Commun. Mass Spectrom.* **18**: 1561–1568.
- CASCIOTTI, K. L. 2002. Molecular and stable isotopic characterization of enzymes involved in nitrification and nitrifier-denitrification. Ph.D. thesis. Princeton Univ.
- , D. M. SIGMAN, M. GALANTER HASTINGS, J. K. BÖHLKE, AND A. HILKERT. 2002. Measurement of the oxygen isotopic composition of nitrate in seawater and freshwater using the denitrifier method. *Anal. Chem.* **74**: 4905–4912.
- , ———, AND B. B. WARD. 2003. Linking diversity and stable isotope fractionation in ammonia-oxidizing bacteria. *Geomicrobiol. J.* **20**: 335–353.
- DELONG, E. F., G. S. WICKMAN, AND N. R. PACE. 1989. Phylogenetic stains: Ribosomal RNA-based probes for the identification of single cells. *Science* **243**: 1360–1363.

- DORAN, P. T., C. P. MCKAY, G. D. CLOW, G. L. DANA, A. G. FOUNTAIN, T. NYLEN, AND W. B. LYONS. 2002. Valley floor climate observations from the McMurdo dry valleys, Antarctica, 1986–2000. *J. Geophys. Res.* **107**: 4772, doi:10.1029/2001JD002045.
- DORE, J. E., B. N. POPP, D. M. KARL, AND F. J. SANSONE. 1998. A large source of atmospheric nitrous oxide from subtropical North Pacific surface waters. *Nature* **396**: 63–66.
- DOWNES, M. T. 1988. Aquatic nitrogen transformations at low oxygen concentrations. *Appl. Environ. Microbiol.* **54**: 172–175.
- FLÄRDH, K., P. S. COHEN, AND S. KJELLEBERG. 1992. Ribosomes exist in large excess over the apparent demand for protein synthesis during carbon starvation in marine *Vibrio* sp. Strain CCUG 15956. *J. Bacteriol.* **174**: 6780–6788.
- FOREMAN, C. M., C. F. WOLF, AND J. C. PRISCU. 2004. Impact of episodic warming events on the physical, chemical and biological relationships of lakes in the McMurdo Dry Valleys, Antarctica. *Aquat. Geochem.* **10**: 239–268.
- FREITAG, T. E., AND J. I. PROSSER. 2003. Community structure of ammonia-oxidizing bacteria within anoxic marine sediments. *Appl. Environ. Microbiol.* **69**: 1359–1371.
- , AND ———. 2004. Differences between betaproteobacterial ammonia-oxidizing communities in marine sediments and those in overlying water. *Appl. Environ. Microbiol.* **70**: 3789–3793.
- GLATZ, R. E., P. W. LEPP, B. B. WARD, AND C. A. FRANCIS. 2006. Planktonic microbial community composition across steep physical/chemical gradients in permanently ice-covered Lake Bonney, Antarctica. *Geobiology* **4**: 53–67.
- GOREAU, T. J., W. A. KAPLAN, S. C. WOFSEY, M. B. MCELROY, F. W. VALOIS, AND S. W. WATSON. 1980. Production of NO₂⁻ and N₂O by nitrifying bacteria at reduced concentrations of oxygen. *Appl. Environ. Microbiol.* **40**: 526–532.
- HOLMES, R. M., J. W. MCCLELLAND, D. M. SIGMAN, B. FRY, AND B. J. PETERSON. 1998. Measuring ¹⁵N-NH₄⁺ in marine, estuarine and fresh waters: An adaptation of the ammonia diffusion method for samples with low ammonium concentrations. *Mar. Chem.* **60**: 235–243.
- KIM, K.-R., AND H. CRAIG. 1993. Nitrogen-15 and oxygen-18 characteristics of nitrous oxide: A global perspective. *Science* **262**: 1855–1857.
- KÖNNEKE, M., A. E. BERNHARD, J. R. DE LA TORRE, C. B. WALKER, J. B. WATERBURY, AND D. A. STAHL. 2005. Isolation of an autotrophic ammonia-oxidizing marine archaeon. *Nature* **437**: 543–546.
- LANE, D. J. 1991. 16S/23S rRNA sequencing, p. 115–175. *In* E. Stackebrandt and M. Goodfellow [eds.], *Nucleic acid techniques in bacterial systematics*. Wiley Press.
- LEE, P. A., AND OTHERS. 2004. Thermodynamic constraints on microbially mediated processes in lakes of the McMurdo Dry Valleys, Antarctica. *Geomicrobiol. J.* **21**: 1–17.
- LYONS, W. B., S. K. FRAPE, AND K. A. WELCH. 1999. History of McMurdo Dry Valley lakes, Antarctica, from stable chlorine isotope data. *Geology* **27**: 527–530.
- , S. W. TYLER, R. A. WHARTON, D. M. MCKNIGHT, AND B. H. VAUGHN. 1998a. A late Holocene desiccation of Lake Hoare and Lake Fryxell, McMurdo Dry Valleys, Antarctica. *Antarct. Sci.* **10**: 247–256.
- , K. A. WELCH, AND P. SHARMA. 1998b. Chlorine-36 in the waters of the McMurdo Dry Valley lakes, southern Victoria Land, Antarctica: Revisited. *Geochim. Cosmochim. Acta.* **62**: 185–191.
- MATSUBAYA, O., H. SAKAI, T. TORII, H. BURTON, AND K. KERRY. 1979. Antarctic saline lakes—stable isotope ratios, chemical compositions and evolution. *Geochim. Cosmochim. Acta* **43**: 7–25.
- MISKIN, I. P., P. FARRIMOND, AND I. M. HEAD. 1999. Identification of novel bacterial lineages as active members of microbial populations in a freshwater sediment using a rapid RNA extraction procedure and RT-PCR. *Microbiol.-UK* **145**: 1977–1987.
- NAQVI, S. W. A. 1991. N₂O production in the ocean. *Nature* **349**: 373–374.
- OSTROM, N. E., A. PITT, R. SUTKA, P. H. OSTROM, A. S. GRANDY, K. M. HUIZINGA, AND G. P. ROBERTSON. 2007. Isotopologue effects during N₂O reduction in soils and in pure cultures of denitrifiers. *J. Geophys. Res.* **112**: G02005, doi:10.1029/2006JG000287.
- , M. E. RUSS, B. POPP, T. M. RUST, AND D. M. KARL. 2000. Mechanisms of nitrous oxide production in the subtropical North Pacific based on determinations of the isotopic abundances of nitrous oxide and di-oxygen. *Chemosphere Global Change Sci.* **2**: 281–290.
- PÉREZ, T., S. E. TRUMBORE, S. C. TYLER, P. A. MATSON, I. ORTIZ-MONASTERIO, T. RAHN, AND D. W. T. GRIFFITH. 2001. Identifying the agricultural imprint on the global N₂O budget using stable isotopes. *J. Geophys. Res.* **106**: 9869–9878.
- POREDA, R. J., A. G. HUNT, W. B. LYONS, AND K. A. WELCH. 2004. The helium isotopic chemistry of Lake Bonney, Taylor Valley, Antarctica: Timing of late Holocene climate change in Antarctica. *Aquat. Geochem.* **10**: 353–371.
- PRISCU, J. C. 1995. Phytoplankton nutrient deficiency in lakes of the McMurdo dry valleys, Antarctica. *Freshw. Biol.* **34**: 215–227.
- . 1997. The biogeochemistry of nitrous oxide in permanently ice-covered lakes of the McMurdo Dry Valleys, Antarctica. *Global Change Biol.* **3**: 301–315.
- , M. T. DOWNES, AND C. P. MCKAY. 1996. Extreme supersaturation of nitrous oxide in a poorly ventilated Antarctic lake. *Limnol. Oceanogr.* **41**: 1544–1551.
- REVSBECH, N. P., N. RISGAARD-PETERSEN, A. SCHRAMM, AND L. P. NIELSEN. 2006. Nitrogen transformations in stratified aquatic microbial ecosystems. *Antonie van Leeuwenhoek* **90**: 361–375.
- RÖLING, F. M., AND I. M. HEAD. 2005. Prokaryotic systematics: PCR and sequence analysis of amplified 16S rRNA genes, p. 25–63. *In* A. M. Osborn and C. J. Smith [eds.], *Molecular microbial ecology*. Taylor and Francis.
- SAMUELSSON, M.-O. 1985. Dissimilatory nitrate reduction to nitrite, nitrous oxide, and ammonium by *Pseudomonas putrefaciens*. *Appl. Environ. Microbiol.* **50**: 812–815.
- SIGMAN, D. M., K. L. CASCIOTTI, M. ANDREANI, C. BARFORD, M. GALANTER, AND J. K. BÖHLKE. 2001. A bacterial method for the nitrogen isotopic analysis of nitrate in seawater and freshwater. *Anal. Chem.* **73**: 4145–4153.
- SPIGEL, R. H., AND J. C. PRISCU. 1996. Evolution of temperature and salt structure of Lake Bonney, a chemically stratified Antarctic lake. *Hydrobiologia* **321**: 177–190.
- , AND ———. 1998. Physical limnology of the McMurdo Dry Valleys Lakes, p. 153–187. *In* J. C. Priscu [ed.], *Ecosystem dynamics in a polar desert: The McMurdo Dry Valleys, Antarctica*. American Geophysical Union.
- STEIN, L. Y., AND Y. L. YUNG. 2003. Production, isotopic composition, and atmospheric fate of biologically produced nitrous oxide. *Annu. Rev. Earth Planet. Sci.* **31**: 329–356.
- SUTKA, R. L., N. E. OSTROM, P. H. OSTROM, J. A. BREZNAK, H. GANDHI, A. J. PITT, AND F. LI. 2006. Distinguishing nitrous oxide production from nitrification and denitrification on the basis of isotopomer abundances. *Appl. Environ. Microbiol.* **72**: 638–644.
- TOYODA, S., AND N. YOSHIDA. 1999. Determination of nitrogen isotopomers of nitrous oxide on a modified isotope ratio mass spectrometer. *Anal. Chem.* **71**: 4711–4718.

- VINCENT, W. F., M. T. DOWNES, AND C. L. VINCENT. 1981. Nitrous oxide cycling in Lake Vanda, Antarctica. *Nature* **292**: 618–620.
- VOYTEK, M. A., AND B. B. WARD. 1995. Detection of ammonium-oxidizing bacteria of the beta-subclass proteobacteria in aquatic samples with the PCR. *Appl. Environ. Microbiol.* **61**: 1444–1450.
- , ———, AND J. C. PRISCU. 1998. The abundance of ammonium-oxidizing bacteria in L. Bonney, Antarctica determined by immunofluorescence, PCR, and in situ hybridization, p. 217–228. *In* J. C. Priscu [ed.], *Ecosystem dynamics in a polar desert: The McMurdo Dry Valleys, Antarctica*. American Geophysical Union.
- WAGNER, M., G. RATH, R. AMANN, H.-P. KOOPS, AND K.-H. SCHLEIFER. 1995. In situ identification of ammonia-oxidizing bacteria. *Syst. Appl. Microbiol.* **18**: 251–264.
- WARD, B. B., J. GRANGER, M. T. MALDONADO, K. L. CASCIOTTI, S. HARRIS, AND M. L. WELLS. 2005. Denitrification in the hypolimnion of permanently ice-covered Lake Bonney, Antarctica. *Aquat. Microb. Ecol.* **38**: 295–307.
- , ———, ———, AND M. L. WELLS. 2003. What limits bacterial production in the suboxic region of permanently ice-covered Lake Bonney, Antarctica? *Aquat. Microb. Ecol.* **31**: 33–47.
- , AND J. C. PRISCU. 1997. Detection and characterization of denitrifying bacteria from a permanently ice-covered Antarctic lake. *Hydrobiologia* **347**: 57–68.
- WEATHERS, P. J. 1984. N₂O evolution by green algae. *Appl. Environ. Microbiol.* **48**: 1251–1253.
- WESTLEY, M. B., B. N. POPP, AND T. M. RUST. 2007. The calibration of the intramolecular nitrogen isotope distribution in nitrous oxide measured by isotope ratio mass spectrometry. *Rapid Commun. Mass Spectrom.* **21**: 391–405.
- WRAGE, N., G. L. VELTHOF, M. L. VAN BEUSICHEM, AND O. OENEMA. 2001. Role of nitrifier denitrification in the production of nitrous oxide. *Soil Biol. Biochem.* **33**: 1723–1732.
- YAMULKI, S., S. TOYODA, N. YOSHIDA, E. VALDKAMP, B. GRANT, AND R. BOL. 2001. Diurnal fluxes and the isotopomer ratios of N₂O in a temperate grassland following urine amendment. *Rapid Commun. Mass Spectrom.* **15**: 1263–1269.
- YOSHIDA, N. 1988. ¹⁵N-depleted N₂O as a product of nitrification. *Nature* **335**: 528–529.
- , AND S. TOYODA. 2000. Constraining the atmospheric N₂O budget from intramolecular site preference in N₂O isotopomers. *Nature* **405**: 330–334.
- YOSHINARI, T., M. A. ALTABET, S. W. A. NAQVI, L. CODISPOTI, A. JAYAKUMAR, M. KUHLAND, AND A. DEVOL. 1997. Nitrogen and oxygen isotopic composition of N₂O from suboxic waters of the eastern tropical North Pacific and the Arabian Sea—measurement by continuous flow isotope-ratio monitoring. *Mar. Chem.* **56**: 253–264.

Received: 30 June 2007
Accepted: 20 May 2008
Amended: 26 July 2008